Semiconductor Strain Transducers

By F. T. GEYLING and J. J. FORST

(Manuscript received February 9, 1960)

The relatively recent discovery of the high piezoresistive sensitivity of semiconductors such as germanium and silicon has made miniature strain transducers available that compare with piezoelectric devices in dynamic applications but are also capable of producing dc signals After a historical survey of research in piezoresistivity, a brief phenomenological description of the physical effect is given and the pertinent solid state theory is summarized. Various applications of semiconductor elements as strain transducers are then discussed in detail, special emphasis being given to surface strain gages. The problems of maximizing the bond rigidity for such gages and compensating for temperature effects are dealt with, and future efforts in these directions are outlined.

I. INTRODUCTION

Around the end of 1958, considerable interest developed among experimenters and transducer manufacturers in the possible application of highly sensitive piezoresistive elements as subminiature sensing devices for displacements, strains and forces. For dynamic problems, piezoelectric pickups consisting of quartz or barium titanate had previously found their way into numerous applications for the measurement of vibrations, shock intensities and stress waves. However, similar lightweight instruments that could handle dc or near-dc signals as well as dynamic ones were yet to be found. Piezoresistive semiconductor materials do just that. The present paper is intended to give a summary of established facts about them and indicate some of their potentialities.

The history of research in piezoresistive phenomena dates back to the 1920's, when some of the earliest observations were made by Bridgman on single and polycrystalline metal specimens.[1,2] These results were augmented by several contributions in the 1930's from Allen and Cookson,[3-7] who measured the effects that were subsequently utilized in wire strain gages. To the authors' knowledge, the first piezoresistive measure-

ments on semiconductors were made in 1953 in connection with basic research for the transistor technology.[8,9] From this point on, further investigations of piezoresistance in semiconductors were carried on very actively in an experimental direction[10-15] and along theoretical lines.[13,16,17] Shortly after the original measurements, efforts were made toward applications of the phenomenon, and these have continued ever since as one of the device technologies that evolved from the original work in transistor development.[18-26]

We begin this review with a simplified account of the essential solid state theory and its experimental corroborations. This sketch of existing knowledge is intended for the experimentalist concerned with strain transducers and does not make any claims regarding novelty. It merely outlines the basic thoughts and gives references for additional detail. The remainder of the paper covers several applications of piezoresistive transducers at room temperature, and then proceeds to a discussion of strain gage applications at various temperatures.

The authors are indebted to W. P. Mason, C. Herring, R. N. Thurston, R. O'Regan, J. S. Courtney-Pratt, and W. L. Feldmann for help and suggestions, and to several previous authors in this field for permission to use some of the material listed in the references at the end of this paper.

II. PIEZORESISTIVE PROPERTIES OF SEMICONDUCTORS

2.1 *Phenomenological Description*

From routine applications of Ohm's law, we are used to thinking of the relation between potential difference and current as involving only a scalar constant of proportionality, the resistance, between the vectors **V** and **I**. This is trivially obvious for a unidimensional conductor such as a link in some circuit. If we restate the situation for conduction in a three-dimensional medium, however, then the current density vector, **i**, generated by a potential gradient, **E**, will not in general have the same direction as the latter unless the medium is isotropic or cubic; i.e., $\mathbf{i} = (1/\rho)\mathbf{E}$ if the resistivity ρ is the same in all directions within the conductor. For monocrystalline conductors this is not necessarily the case; i.e., the current vector resulting from an impressed voltage gradient is not colinear with the latter and, conversely, if some specified **i** is maintained in the material the attendant **E** is not colinear with it. We may formulate this situation more concisely by identifying the components of **E** and **i** with numeric subscripts indicating the directions of orthogonal crystal axes. Then $E_1 = \rho_{11}i_1 + \rho_{12}i_2 + \rho_{13}i_3$, etc., where the first sub-

script for each ρ_{ij} indicates the field component it is contributing to, and the second subscript identifies the current component making the contribution. In literal notation and using the summation convention, we have

$$E_i = \rho_{ij} i_j , \tag{1}$$

where all subscripts have the range 1 to 3. Only if $\rho_{ij} = 0$ for $i \neq j$ and $\rho_{11} = \rho_{22} = \rho_{33} = \rho$ does the medium provide isotropic conduction. Such is indeed the case for unstressed germanium and silicon, which possess a cubic crystal structure.

We now generalize the relation (1) to allow for piezoresistive effects due to a set of stresses T_{kl}, where T_{11}, T_{22}, T_{33} are normal stresses along crystal axes and T_{12}, T_{13}, T_{23} the shear stresses in this coordinate system. Then,

$$E_i = \rho_{ij} i_j + \pi_{ijkl} i_j T_{kl} , \tag{2}$$

where $\pi_{ijkl} T_{kl}$ are the stress-dependent contributions to the resistivity. The proportionality constants π are characterized not only by i and j, as was the zero-stress resistivity, but also by k and l, which relate each of them to a particular stress component T_{kl}. Clearly, (2) could be treated as a tensor relation, but, since we do not expect to carry out many operations on it during the following discussion, not much would be gained from this formalism. We shall, however, find it convenient to use the following contractions for various combinations of subscript values:

$$11 \sim 1,$$
$$22 \sim 2,$$
$$33 \sim 3,$$
$$23 \sim 4,$$
$$13 \sim 5,$$
$$12 \sim 6.$$

Utilizing the fact that the zero-stress resistivity for germanium and silicon is isotropic, we now introduce a new set of piezoresistance coefficients π_{st} such that, for example,

$$\rho\pi_{11} = \pi_{1111} ; \qquad \rho\pi_{12} = \pi_{1122} ; \qquad \rho\pi_{44} = 2\pi_{2323} .$$

If one finally observes all the symmetry conditions and the vanishing of certain π_{st},[20] one finds the following array for them:

$s\backslash t$	1	2	3	4	5	6
1	π_{11}	π_{12}	π_{12}	0	0	0
2	π_{12}	π_{11}	π_{12}	0	0	0
3	π_{12}	π_{12}	π_{11}	0	0	0
4	0	0	0	π_{44}	0	0
5	0	0	0	0	π_{44}	0
6	0	0	0	0	0	π_{44}.

(3)

The explicit form of (2) then becomes

$$\frac{E_1}{\rho} = i_1[1 + \pi_{11}T_1 + \pi_{12}(T_2 + T_3)] + \pi_{44}(i_2T_6 + i_3T_5),$$

$$\frac{E_2}{\rho} = i_2[1 + \pi_{11}T_2 + \pi_{12}(T_1 + T_3)] + \pi_{44}(i_1T_6 + i_3T_4), \tag{4}$$

$$\frac{E_3}{\rho} = i_3[1 + \pi_{11}T_3 + \pi_{12}(T_1 + T_2)] + \pi_{44}(i_1T_5 + i_2T_4).$$

We note that the second terms in the right-hand sides, $\pi_{11}T_1i_1$, $\pi_{11}T_2i_2$ or $\pi_{11}T_3i_3$, represent the piezoresistive effect as we know it from wire and foil gages. It is the effect of a stress in the direction of current flow on the potential drop in that direction. The additional terms in (4) simply reflect the more complicated behavior of the stressed lattice, which exhibits piezoresistive "carry-over" into E_i from stress components other than T_i.

In many applications of semiconductor transducers one is indeed concerned with the relation between a uniaxial state of stress T' and i' and E' in the same direction, where the latter, however, is not necessarily along a crystal axis, but exhibits the direction cosines l, m, n with respect to 1, 2, 3. The desired relation, based on the fundamental ones in (4), follows from

$$i_1 = li', \qquad i_2 = mi', \qquad i_3 = ni';$$

$$T_{11} = l^2T', \qquad T_{22} = m^2T', \qquad T_{33} = n^2T';$$

and

$$T_{12} = lmT', \qquad T_{13} = lnT', \qquad T_{23} = mnT';$$

which we substitute into (4). Using the results in

$$E' = lE_1 + mE_2 + nE_3 ,$$

we can obtain

$$\begin{aligned} \frac{E'}{\rho} &= i'\{1 + T'[\pi_{11} + 2(\pi_{44} + \pi_{12} - \pi_{11})(l^2m^2 + l^2n^2 + m^2n^2)]\} \\ &= i'[1 + \pi_l T']. \end{aligned} \tag{5}$$

If $(\pi_{44} + \pi_{12} - \pi_{11}) \neq 0$ and π_{11} and $(\pi_{44} + \pi_{12} - \pi_{11})$ have the same sign, or if $| \pi_{44} + \pi_{12} - \pi_{11} | > 3 | \pi_{11} |$, it can be shown that $| \pi_l |$ exhibits maxima at $l = m = n = \pm\sqrt{\frac{1}{3}}$, i.e., along the [111] axes. Otherwise, the maxima occur along the crystal axes.

Besides uniaxial stress in the [111] direction, we shall be interested in the effects of shear stresses T_4, T_5, T_6 alone. We observe from (4) that they produce a piezoresistive effect by virtue of π_{44}. In the event of hydrostatic pressure, finally, we note that $T_1 = T_2 = T_3 = -p$ and $T_4 = T_5 = T_6 = 0$, so that

$$\mathbf{E} = \rho\mathbf{i}[1 - p(\pi_{11} + 2\pi_{12})]. \tag{6}$$

Some typical values for the adiabatic piezoresistive coefficients of germanium and silicon at room temperature are given in Table I.[9]

The dimensions for the π follow from (4). $(m_l)_{111}$ is a so-called elastoresistive coefficient, which is computed from $(\pi_l)_{111}$ by means of Young's modulus in the [111] direction. Since it represents $\Delta\rho/\rho\epsilon$, where ϵ is the strain in the [111] direction, it is analogous to the "gage factor" defined for strain gages of the wire or foil type. We note that all these factors in the above table are considerably larger than a typical value of 2 for commercially available strain gages. This explains the current interest

TABLE I

Material	ρ, in ohm-cm	π, in 10^{-12} cm² per dyne				$(m_l)_{111}$, dimensionless
		π_{11}	π_{12}	π_{44}	$(\pi_l)_{111}$	
Germanium, n-type..	16.6	−5.2	−5.5	−138.7	−101.2	−157
Germanium, p-type..	1.1	−3.7	+3.2	+96.7	+65.4	+101.5
Silicon, p-type.......	7.8	+6.6	−1.1	+138.1	+93.6	+175
Silicon, n-type.......	11.7	−102.2	+53.4	−13.6	−7.6	−133

in semiconductor gages for applications around 25°C and possibly at elevated temperatures. We also notice that the first three materials in the table possess rather small π_{11} and π_{12} in contrast to π_{44}. For n-type silicon the situation is, however, reversed. The coefficient for hydrostatic loading, $\pi_{11} + 2\pi_{12}$ according to (6), is rather negligible in all of these semiconductors. We finally observe that all entries in the table are for bulk materials; i.e., they do not account for dimensional changes of a transducer due to applied strain. In the following, we sketch the explanation of these phenomena by solid state theory.

2.2 *Physical Explanation*

Fig. 1 illustrates some of the simplest ideas concerning the lattice structures of crystals. Although modern theories combine the concepts of statistics and quantum mechanics to represent the motion and energy content of a particle by wave functions, it will be adequate for a plausible description of piezoresistance to think of electrons in a corpuscular fashion. Fig. 1(a) illustrates the process by which "holes" and free electrons are generated or cancelled in a lattice structure by separation of an electron from its regular location in the structure of lattice bonds or by its "falling into" some "open" bond. In the lower left part of the figure we indicate the energy of the freely moving electron as that of the

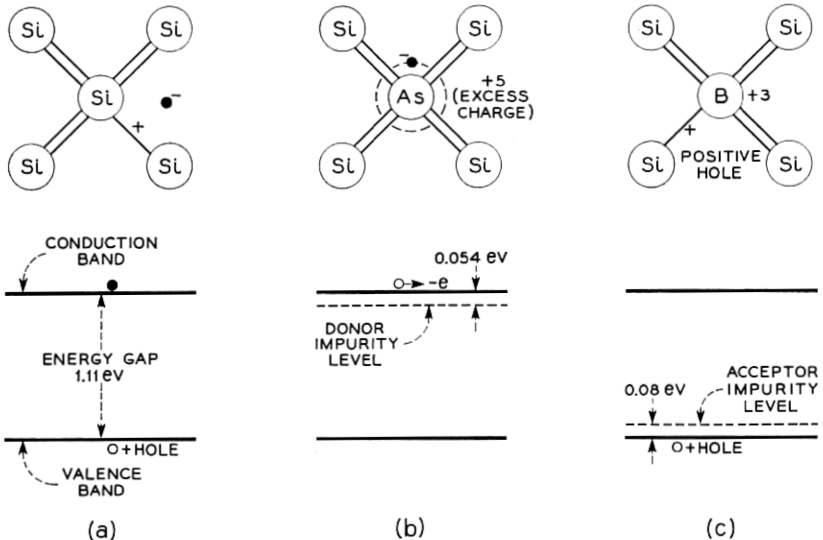

Fig. 1 — Schematic diagram of solid state lattice.

conduction band and the energy level in a closed bond as the *valence band*. The differential energy (1.11 ev for a silicon lattice) is liberated in the cancellation or absorbed in the generation of an open bond. Fig. 1(b) illustrates the state of affairs in the presence of a "donor" impurity in the lattice whose extra charge (one electron for arsenic) lacks relatively little energy (0.054 ev) to be raised into the conduction band and become a free electron. Conversely, the presence of an "acceptor" impurity offers an open-bond level which could be reached by some valence electron at the absorption of very little energy (0.08 ev for boron as acceptor), thus leaving a hole in its original location. These two processes constitute the basic transport phenomena in semiconductors.

Consider now in more detail the energy state of an electron in or above the conduction band. Quantum mechanics permits us to associate separate wave numbers $k_{1,2,3}$ with the components of its motion in the directions 1, 2, 3. In some media (e.g. a silicon lattice) it is possible for an electron to achieve a minimum energy which it requires to remain in the conduction band by several combinations of k_1, k_2 and k_3. These combinations are referred to as *band edge points*, since they constitute lower bounds for the energy required of a free electron. Fig. 2 shows such points in "k-space" for n-type silicon, where this space is resolved into components corresponding to the directions of crystal axes. An electron

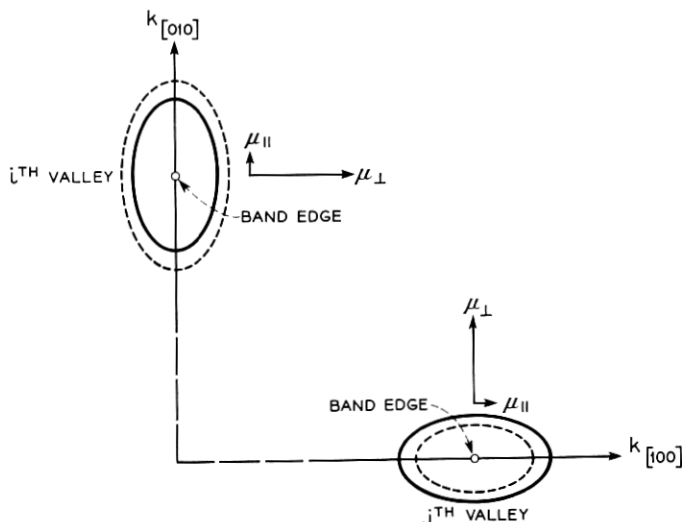

Fig. 2 — Constant energy surfaces in k-space.

with slightly more energy than is required at a band edge point may possess such energy by a variety of combinations in $k_{1,2,3}$ that describe a constant-energy surface about the band edge point. A family of such surfaces, centered on a band edge point, describes a so-called *energy valley* in k-space. In the case of silicon and germanium, these families consist of prolate ellipsoids of revolution that are aligned with the crystal axes. Since there are several band edge points, we speak of a *multivalley model.* The fact that the constant energy surfaces possess principal axes of unequal lengths may be interpreted to mean that the components of effective mass and mobility, $\mu_{1,2,3}$, of an electron or the components of conductivity, $\sigma_{1,2,3}$, in such a valley are different in the three principal directions. (In Fig. 2 we indicate mobility parallel to a crystal axes by $\mu_{\parallel}$ and transverse to the axis by $\mu_{\perp}$.) Consequently, these electrons make anisotropic contributions to the total conductivity of the lattice. If, however, all ellipsoids have the same proportions and all valleys are equally populated with electrons, the over-all conductivity of the lattice will be isotropic, as we have already observed for silicon and germanium in the unstressed state. The formulation of the above ideas in mathematical terms is known as *mobility theory.** While this theory is advanced enough to account for the effects of impurity concentration, it also gives an adequate explanation of the variations of zero-stress resistivity with temperature (see Fig. 4 of Ref. 16). An experimental family of resistivity versus temperature characteristics for n-type silicon with various concentrations of phosphorus impurities is given in Fig. 3.

The theoretical treatment of piezoresistance now proceeds from the ideas of the multivalley model. It can be shown that the application of an anisotropic stress condition changes the relative energies, and hence changes the populations of these valleys. Thus, if a lattice started out as an isotropic conductor due to equal populations in the valleys at zero stress, an anisotropy is impressed on the total conductivity in the stressed state by the valleys which now attract the majority of electrons. Again, these ideas are treated in full detail in Ref. 16 (pp. 251–258 and Appendix C) and the resulting expressions for π_{st} yield relative magnitudes that are in essential agreement with Table I. Since the present theory

* Our lattice model serving as a basis for this theory is really a so-called simple multivalley model, in contrast to so-called degenerate single and multivalley models where the families of constant energy surfaces possess branch points. The relaxation time, τ, connected with electron mobility is only assumed to be a function of energy so that Maxwellian statistics are applicable. This simplification is adequate for a treatment of intra- and intervalley scattering due to acoustic excitation and neutral impurities, but not for cases involving highly anisotropic effective masses and subject to ionized-impurity scattering. A full treatment of this theory is given in Refs. 16 and 17.

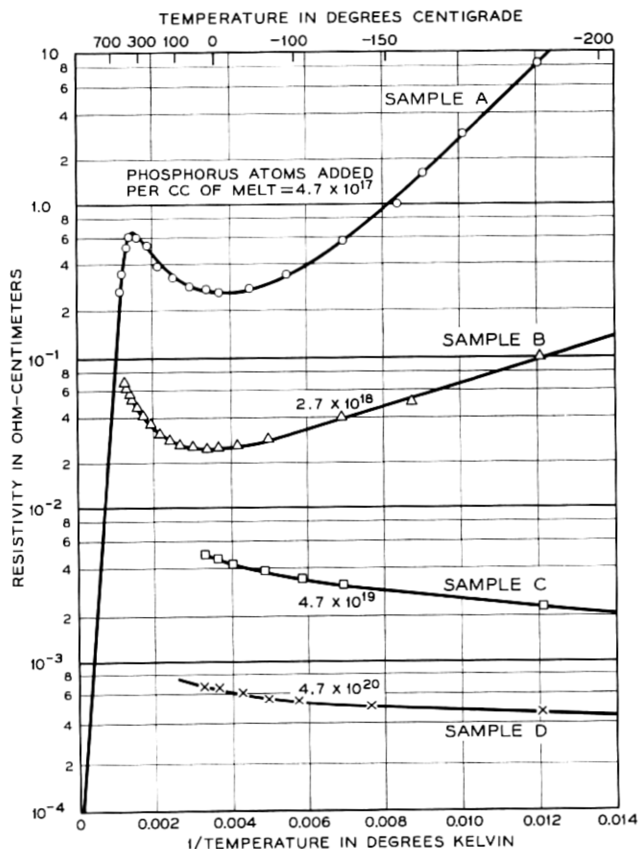

Fig. 3 — Resistivity vs. temperature for n-type silicon (from Ref. 27).

neglects certain minor effects of strain on the conductivity, it predicts that dilations along [100] directions will produce no piezoresistive effect in lattices with valleys on [111] axes since by symmetry the effect of the strain is the same on each valley. By the same token, no aggregative effect will be observed from strain in the [111] direction on material with valleys in the [100] direction. In the former case $\pi_{11} - \pi_{12} = 0$ and in the latter $\pi_{44} = 0$. Allowing for the fact that, in the absence of simplifications, no exact zeros will occur among piezoresistive coefficients, we observe from the experimental data in Table I that n-type germanium, for example, belongs to the first class, while n-type silicon is of the second kind. The theory also indicates a temperature dependence of π_{st} according to

$1/T$, which is experimentally confirmed for π_{11} in n-type silicon by Fig. 4. (Note that χ has been used only in this figure to indicate stress in place of T' or T_{kl} in order to avoid confusion with temperature, T. The reciprocal temperature dependence is quite exact in the temperature ranges where either intravalley or intervalley scattering predominate. Between these, the dependence is more complicated.)

III. GENERAL APPLICATIONS OF SEMICONDUCTOR STRAIN TRANSDUCERS

In the development of piezoresistive transducers, numerous embodiments other than strain gages had been worked on before the latter were being considered as self-contained units, to be applicable under a

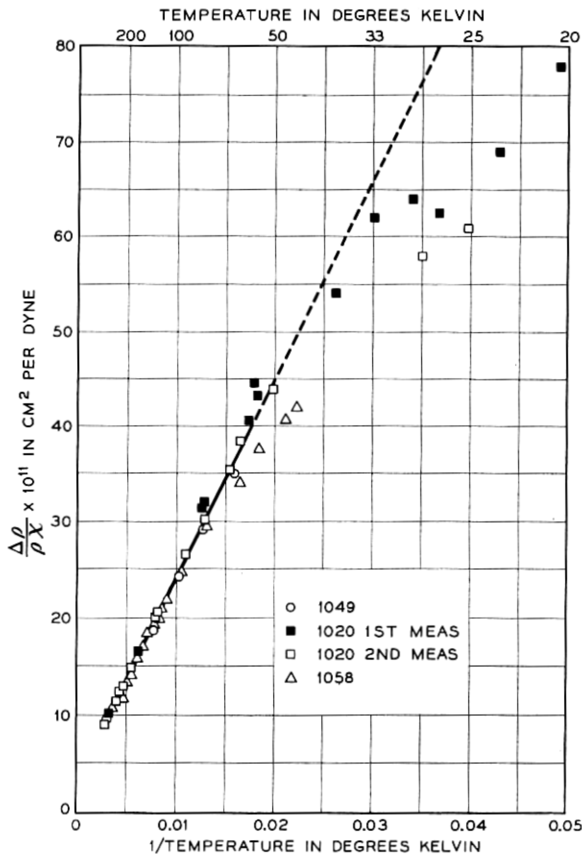

Fig. 4 — Piezoresistive sensitivity vs. temperature for n-type silicon (from Ref. 13).

great variety of test conditions. We shall, therefore, treat these earlier applications in the present section.

To the authors' knowledge, the first use of piezoresistive semiconductor elements for measuring strain was made by Bateman and McSkimin[18] at the suggestion of W. P. Mason, when they constructed a so-called bimorph cantilever unit, consisting of two bonded semiconductor lamellas, to measure small forces acting on the end of this transducer and subjecting it to flexure. By that time it was known that p-type silicon, and p- and n-type germanium exhibit large gage factors in the [111] direction, while n-type silicon is sensitive in the [100] direction, as was shown in Section II. If the circuitry surrounding a transducer is designed to provide a constant bias current, then the voltage change across the element will be the piezoresistive signal and can be expressed as

$$\Delta V = IRG\epsilon, \tag{7}$$

where

I = bias current,
R = nominal resistance of the transducer,
G = gage factor,
ϵ = mechanical strain.

Burns[19] subsequently used bimorph units and elements under axial stress in the construction of microphones. With a bimorph unit, the circuitry of Fig. 5 was employed, where the two elements constitute a tension and a compression arm, respectively, for the bridge, thus dou-

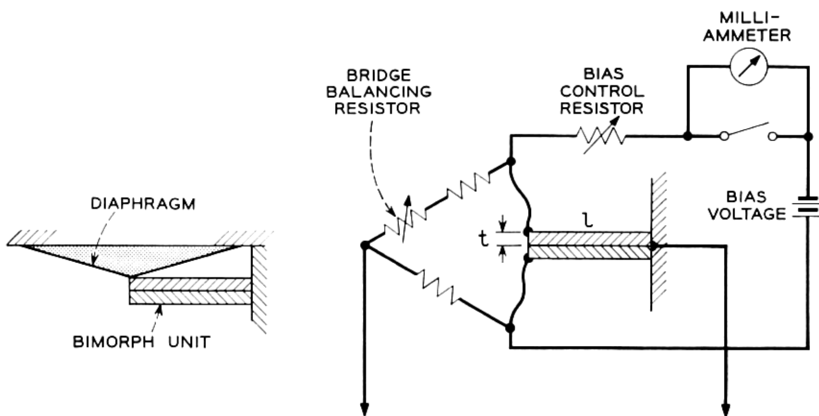

Fig. 5 — Electrical and mechanical arrangement for bimorph microphone (from Ref. 19).

bling the total signal. One pair of diagonal points of the bridge loop was controlled by the external bias circuit, the other served as signal output terminals. In this experimental configuration, the bimorph unit was made to support with one end the apex of a conical diaphragm and was suitably clamped at the other. Electrical connections were made by rhodium-plating the ends of the semiconductors and welding gold wires to them. Armstrong A-1 cement served as an insulating and bonding agent between the two halves of the bimorph unit. In the case of axially loaded elements, the technological details were quite similar, but with the transducer directed normally toward the center of the diaphragm. The dimensioning of both microphone configurations was designed such that the first natural frequency of the instrument was adequately high for practical applications. The merits of a piezoresistive rod microphone lie in the fact that it uses only about one-fiftieth of the power and one-tenth the current required to operate a carbon microphone for the same ac power output from a given acoustic power input.

Further uses of axially loaded and cantilver elements as dynamometers and dilatometers were suggested by Mason and Thurston.[20] In addition, a torsional transducer was developed, as illustrated in Fig. 6(a). It consisted of a cylindrical rod, built in at the left end and subjected to a torque at the right so that T_{yz} was positive on the front ($x > 0$, $z = 0$) and negative on the back ($x < 0$, $z = 0$). If now the transducer is made out of n-type germanium with [100] along the y-axis, and bias currents i_y are transmitted from the electrode 3 to 5 and 6 to 4, then the large piezoresistive shear coefficient π_{44} of this material will produce positive E_z along the front and back of the germanium cylinder; i.e., $E_z = \rho\pi_{44}i_yT_{yz}$ by an adaptation of the third equation in (4). This

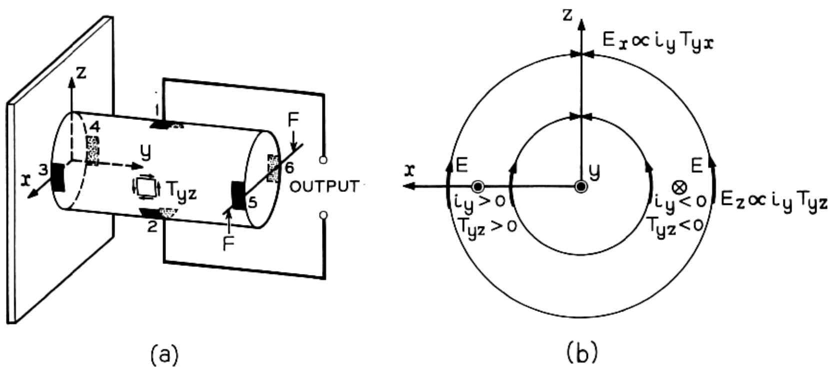

Fig. 6 — Schematic diagram of torsional transducer (from Ref. 20).

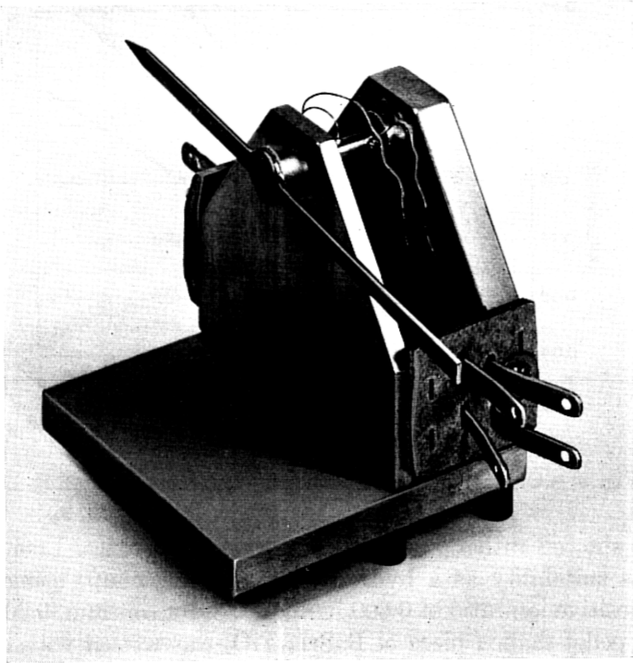

Fig. 7 — Experimental embodiment of torsional transducer (from Ref. 20).

voltage can be read as an output signal between terminals 1 and 2. The spatial relation between i_y, T_{yz} and E_z is illustrated further in Fig. 6(b).

An experimental transducer of this kind is shown in Fig. 7. The right end of the germanium rod is fastened into the upright end plate, while the left end is free to rotate under the torque produced by weights that are hung from the crossarm. Calibration curves for this device under different bias currents are shown in Fig. 8. We note that these data include the effect of cantilever bending in the rod, since the experimental setup subjected the germanium rod to a transverse force in addition to the torque. We also observe that its sensitivity might be improved if the rod were made bimorph with an insulating bonded interface in the yz-plane, which is bridged only by the electrodes 1 and 2. Thus, the parasitic currents from 3 to 4 and 6 to 5 would be eliminated.

Since the work conducted during the thirties on piezoresistive effects under hydrostatic pressure, not much attention had been given to this state of stress as a possible signal generator. In 1956, however, Flaschen, Sauer and Potter[21] discovered that lanthanum-doped barium strontium

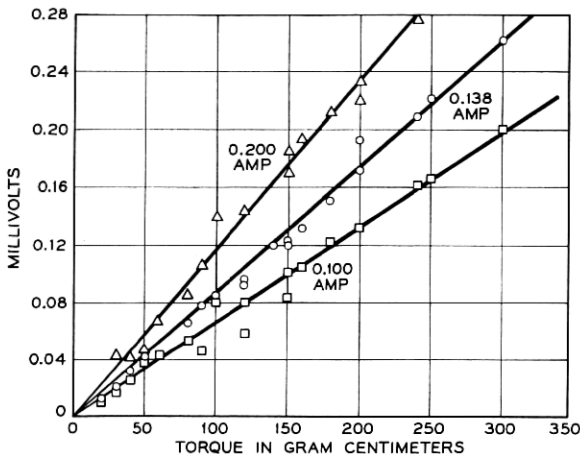

Fig. 8 — Characteristics of torsional transducer (from Ref. 20).

titanate showed rather high piezoresistive sensitivities. Luer[22] investigated its suitability as a hydrostatic pressure pickup, using material with a positive ion ratio of 0.600 barium, 0.397 strontium, 0.003 lanthanum. A pellet-shaped piece of $BaSrLaTiO_2$ was wetted with a layer of indium-gallium amalgam on its top and bottom surfaces and copper terminals were immersed into the amalgam. As an alternative terminating technique, nickel plating could be used to produce a surface to which wire terminals were bonded. Exploratory tests immediately indicated that this transducer was not only pressure sensitive but also showed strong response to temperature changes. Using an ice bath and other precautions, the isothermal calibration curve of Fig. 9 was obtained, which indicates that $\Delta R/R$ per 1000 psi was 2.5 per cent. Thus, the device was about 50 times as sensitive as commercially available load cells. It remains to be seen, however, whether convenient techniques for temperature control or compensation can be developed to make this a versatile miniature pressure gage.

An embodiment of piezoresistive elements for use as an accelerometer has been developed by Courtney-Pratt and Mason.[23] Fig. 10 shows the accelerometer frame with a seismic mass suspended in its center by a pair of sensing elements that are stressed axially in the y-direction. Additional pairs may be added in the x- and z-directions to form a tri-axial transducer.

The use of very small piezoresistive rods, similar to naturally grown whiskers, in dynamometers and extensometers has been pursued further by Forst and Geyling.[24] Fig. 11 shows the way in which germanium

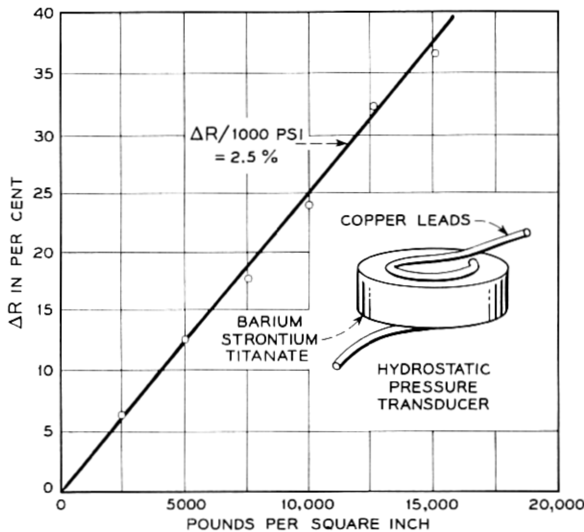

Fig. 9 — Schematic diagram and calibration curve of hydrostatic transducer.

rods with a 0.006-inch-square cross section were cut from an ingot in the [111] direction. After a 0.007-inch slab had been cut from the ingot, this was given a series of notches in the [111] direction and to a depth of 0.006 inch [Fig. 11(c)], whereupon the opposite side of the slab was lapped down until the material separated into the square rods [Fig. 11(d)].* Several ways of attaching gold lead wires to the ends of such

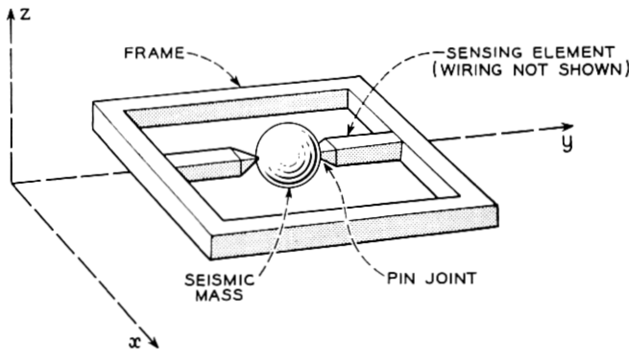

Fig. 10 — Schematic diagram of accelerometer.

* With preliminary equipment it was found advisable to use a slab thickness of 0.015 inch and notch depth of 0.012 inch. The final dimensions of 0.006 × 0.006 inch were then obtained by lapping *both* sides of the work piece in Fig. 11(d).

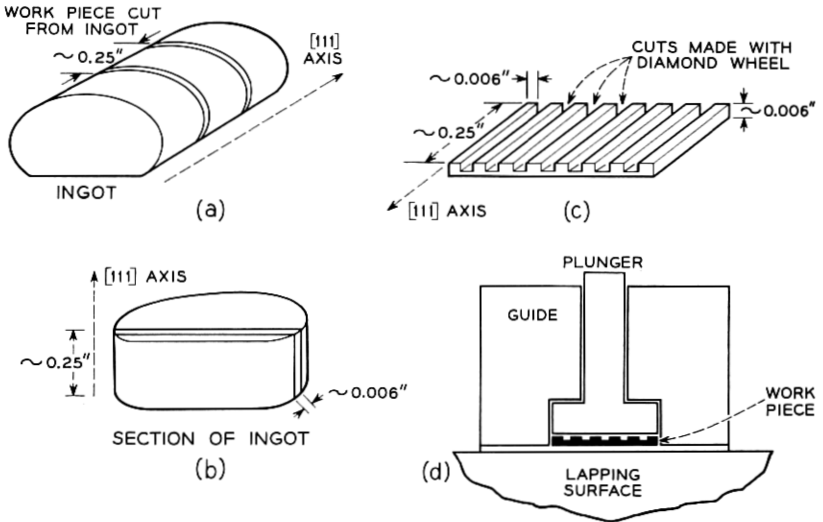

Fig. 11 — Method of cutting germanium rods.

rods were attempted, including such techniques as gold-plating the ends of the rods and then soldering to them, as well as sintered bonds and thermocompression bonds. None of these are fundamentally impossible, and they could be developed into a routine technology. The easiest for laboratory work, however, turned out to be a simple fusion process, which was carried out somewhat above the germanium-gold eutectic temperature. A rod was placed on a piece of flat stock with a pair of gold wires stretched taut across its ends or held down by a retaining spring (Fig. 12) to insure good mechanical contact and to hold the rod in place. Upon heating to 410°C in a nitrogen atmosphere, flow occurred between the germanium and the gold, producing the terminations shown in Fig. 13. Due to a 0.1 per cent doping of antimony in the gold wire,

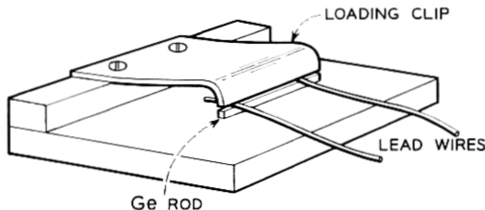

Fig. 12 — Method of fusing gold to germanium.

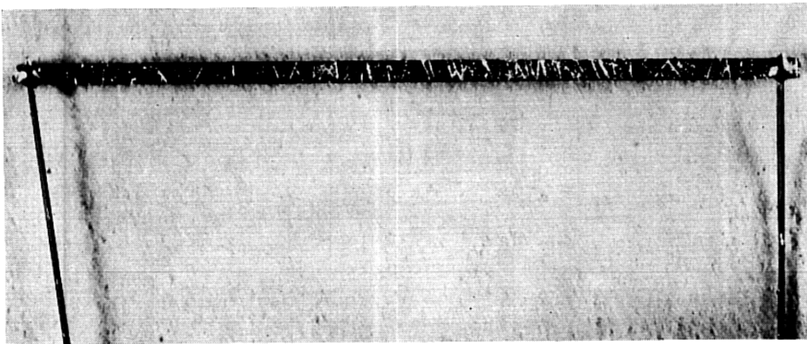

Fig. 13 — Experimental germanium rod and terminations.

these terminations were purely ohmic. As is evident from this discussion, more can be done to mechanize the fabrication of these basic elements and to increase the yield in matched pairs which act as "pickup" and "compensator." Fig. 13 also shows that refined cutting and etching techniques should produce rods with a better surface finish and possibly fewer dislocations, so that the maximum tensile strain in these elements could be increased considerably. At present, the basic techniques are being extended to the use of silicon rods.

The n-type germanium that provided the first experimental elements was manufactured with a zero-stress resistivity of 0.03 ohm-cm, so that a rod of 0.006 × 0.006-inch cross section and 0.25-inch length had a basic resistance of approximately 100 ohms. This was arranged for convenient use of the SR-4 indicator with these elements. Another advantage of this low resistivity lies in the fact that semiconductors with low ρ show less internal contact noise in low-frequency applications than does material with high ρ.

Fig. 14 shows an application of such rods in a tensile extensometer. A tension specimen, h, is held between the grips, g, which transfer the differential motion between gage points on the specimen, i.e., the tensile strain, through the sliding bars f and e to a cantilever-flexing bar of spring steel, k. The structure a,b,c serves to hold the ball bushings, d, which guide the bars f and e. Safety collars, i and i′, on the sliding bars guard against specimen failure. The steel spring, k, carries longitudinal germanium rods on its top and bottom face. These are attached with Araldite CN502 room curing cement, which also serves as insulator. The wiring post, m, supports the lead wires, and the germanium rods are connected into the SR-4 indicator as "active" and "compensating" transducers, to produce twice the signal of a single element.

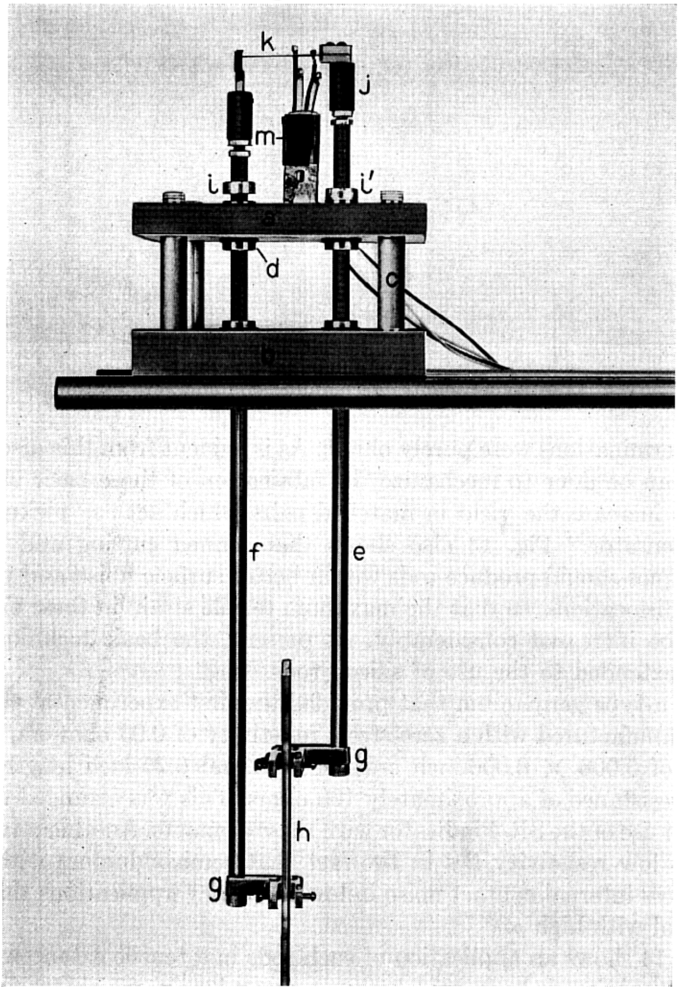

Fig. 14 — Piezoresistive extensometer.

The first experiments immediately showed that these highly sensitive transducers introduced considerable noise into the signal, due to environmental vibrations, draft and varying thermal conditions. Since the present experiment did not call for all the sensitivity available, each element was partially shunted out to reduce its sensitivity to 10 times that of a wire or foil gage and make the noise negligible. Fig. 15 shows typical calibration curves for this extensometer, which were run by controlling

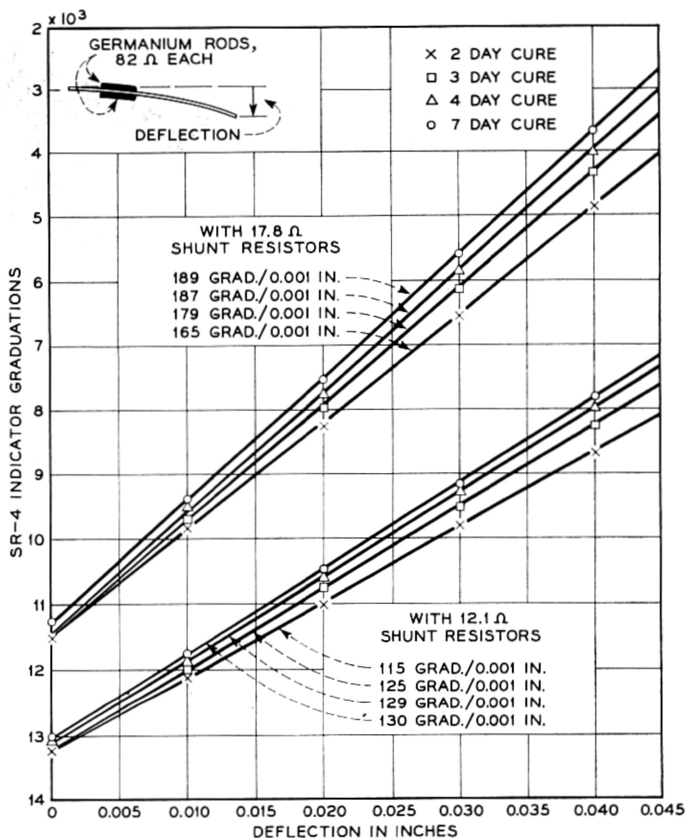

Fig. 15 — Calibration of extensometer.

the relative motion of the gage points, g, with a micrometer and using the arbitrary value of $G = 2$ on the gage factor dial of the indicator. Sensitivities of 189 indicator divisions per mil of extensometer movement and 130 divisions per mil compared favorably with the 14 divisions per mil obtained when A-7 wire gages were used in place of the germanium rods. The shakedown observed in the curves and the fact that some loss of sensitivity occurred with rising ambient temperature indicate that creep and elastic deformation in the bond of the germanium rods is a problem to be kept in mind.[24]

In cases where extremely rigid devices are needed for the measurement of small tensile or compressive forces, the semiconductor elements under axial load are, at present, the only transducers sensitive enough

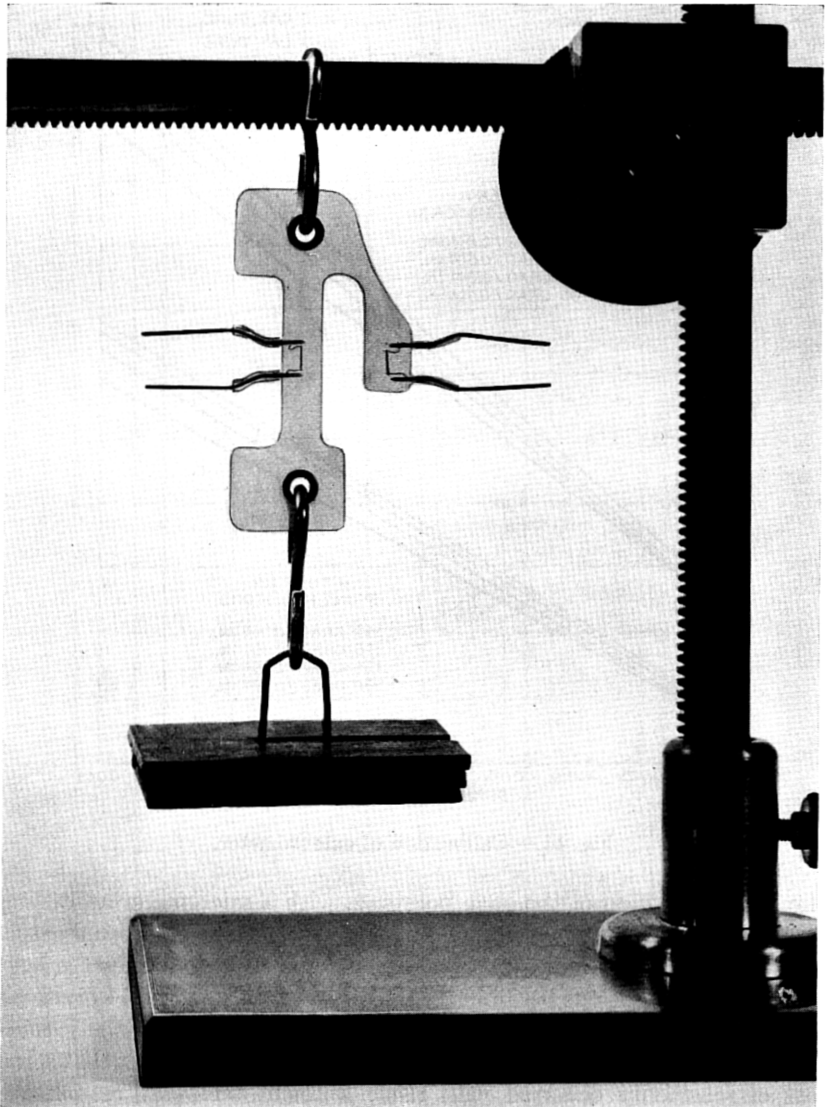

Fig. 16 — Tension dynamometer.

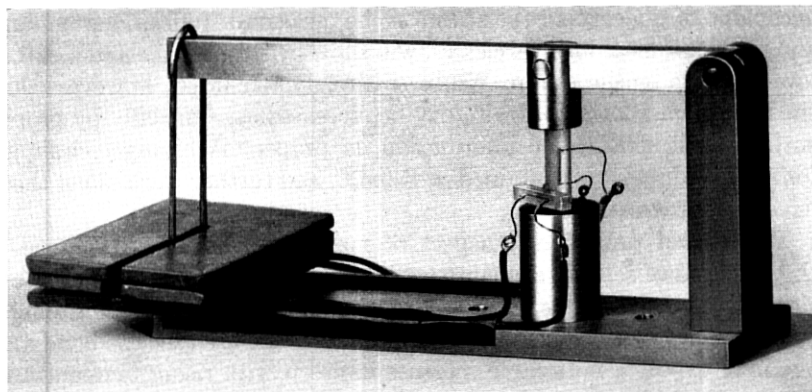

Fig. 17 — Compression dynamometer.

for this purpose. Figs. 16 and 17 show a tension and a compression dynamometer each with an active element in line with the load and the compensator in a monolithic extension of the encapsulation but designed to be strain-free. Typical sensitivities of these transducers were 544 and 637 divisions per pound (with $G = 2.00$ on the indicator). Of course, these sensitivities may be increased further by decreasing the active cross section of the encapsulation.

In closing this section, we note that nearly all the embodiments that were mentioned exhibit negligible deformations in the course of generating a signal. This may be a decisive factor in their application to dynamic problems, where resonances and self-sustained vibrations in the instrumentation must be avoided.

IV. STRAIN GAGE APPLICATIONS

After most of the devices in Section III had been developed,[25] interest shifted to strain gage applications of semiconductor elements. The two main problems in using semiconductor rods for this purpose are: (a) the mechanical one of making a piezoresistive element follow the surface strain of the specimen it is attached to and (b) the task of accurately determining the temperature response of the transducer and compensating for it.

4.1 *Bond Rigidity of Strain Gages*

In order to make a sensing element represent the true deformation of a test model, one must first of all insure that the semiconductor material

is capable of undergoing the strains to be measured. Indeed, germanium and silicon, if machined carelessly, will show little resilience and a rather low ultimate tensile strain. We have already remarked, however, that the maximum allowable strain may be increased substantially by proper surface treatment. Some information on proper machining techniques for semiconductors is contained in Ref. 26, and further work along these lines is in progress.

The second problematic aspect of mechanical gage performance is the adhesion of sensing elements to the model surface. We noted in Section III that some tests (Fig. 15) gave evidence of deformation in the gage cement. This is hardly surprising if resins are used for the bond and one may expect a noticeable increase in creep with rising temperature. For so-called high-temperature applications some special bonding agent will have to be used.

The currently most popular high-temperature cement for strain gages is Allen PBX. It requires a curing cycle with soaking periods at 200°F and 600°F. Since germanium has a thermal coefficient of expansion of $\cong 6 \times 10^{-6}$ per °C and most structural steels have $\alpha \cong 12 \times 10^{-6}$ per °C, some special precautions will be necessary in mounting semiconductor gages on ferrous specimens. Laboratory tests have so far been restricted to Kovar test models where $\alpha = 5 \times 10^{-6}$ per °C, and hence there is little chance of gage failure during the curing cycle. A typical Kovar dumbbell specimen is shown in Fig. 18, and its calibration curve, using p-type silicon rods at room temperature, is given in Fig. 19. The same illustration also lists the sensitivities of these gages at several elevated temperatures.

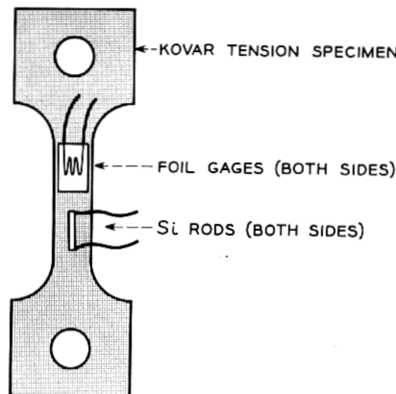

Fig. 18 — Schematic diagram of test specimen for strain gage applications.

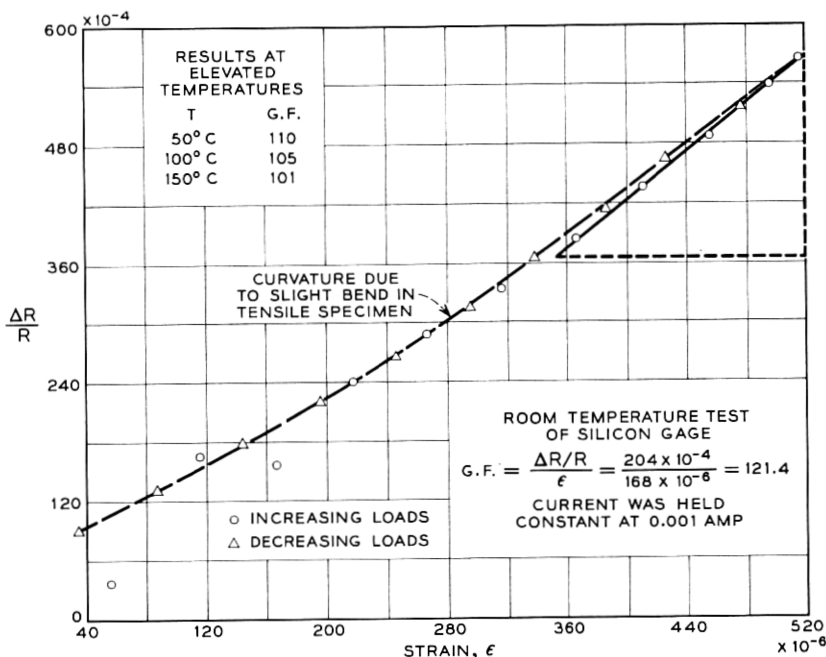

Fig. 19 — Calibration of test specimen for strain gage applications.

One way of observing creep in the bond consists of making measurements of gage signal against time at constant strain in the dumbbell. As an alternative, one may mount a commercial high-temperature gage on the same specimen and, knowing its gage factor, find its strain from the SR-4 signal. If the gage creeps, this value should be less than the strain of the specimen computed from the load. Of course, there is little correlation between the creep of a foil or wire gage and that of a semiconductor rod, since the latter tends to have a smaller ratio of surface to cross-sectional area—even at sizes of 0.001×0.001 inch.* The most reliable, but also the most elaborate, instrumentation for measurements of bond rigidity would consist of placing a suitable mechanical gage (e.g., a Huggenberger tensometer) right on the semiconductor rod and comparing its readings with the computed specimen strain. Needless to say, slippage of a gage would make its apparent gage factor fall below the true one and produce a zero-load signal at the end of a test.

* Clearly, the small size of natural whiskers makes them attractive for the minimization of creep. Their twinning points will add to the bond if they are oriented in a way to permit a snug fit of the whisker against the model surface.

4.2 *Temperature Compensation for Strain Gages*

As we have noted in Section II, the zero-stress resistivity as well as the piezoresistive coefficients of a semiconductor change with temperature. If we are to use these transducers in an extended range around room temperature, not to mention regions like 200°–600°C as required by many applications, both phenomena require compensation.

Fig. 3 indicates the change of ρ with T for n-type silicon, which is the phenomenon one usually eliminates in existing practice by wiring a "dummy" gage into another branch of the bridge as a compensator. This "dummy" needs to be installed near the active gage, preferably on the test model itself, to attain the same ambient conditions, but must remain strain-free. Since these two conditions turn out to be antagonistic in most high-temperature applications, this method ceases to be a satisfactory solution. To aggravate the problem, the high strain sensitivity of semiconductors will magnify the signals from any differential thermal strains between the active and compensating elements over what it is for wire or foil gages.

Several courses of action can be taken in this situation:

i. Subminiature thermocouples are presently on the market that can be installed sufficiently close to each active gage to furnish a temperature signal along with the strain reading. These temperature data can be turned into a correction of the strain reading through the known ρ versus T characteristic of the semiconductor. This may be done either manually or by a compensating adjustment in the indicator circuitry. More elaborate instrumentation might even feature automatic control of this adjustment by a servo.

ii. If the ρ versus T characteristic is difficult to represent with sufficient accuracy in the automatic version of scheme i, we might return to the conventional setup involving a compensating gage. But this element might be contained in a separate furnace whose temperature is automatically steered to match the thermocouple signal from a given active gage.

iii. A third possibility consists of making compensating elements out of semiconductor material with the same ρ versus T characteristic as the active gages but cutting these compensators along the axis of minimum piezoresistive sensitivity ([111] for n-type silicon, and [100] for p-type silicon and p- and n-type germanium). Each gage installation would consist of a closely spaced parallel pair of elements (one "active" and one "dummy"), which are to be wired into opposite branches of the indicator. Thermal signals cancel in the usual way, since cubic lattices exhibit isotropic zero-stress resistivity (i.e., the same ρ on [111]

and [100]), but the greatly different piezoresistive coefficients of the two rods would still produce a large signal due to mechanical strain.

In order to compensate for temperature changes of piezoresistive sensitivity, we observe that the coefficients π_{st} change according to $1/T$. This was shown by Fig. 4 for π_{11} of n-type silicon, where T is in degrees Kelvin. Although the response of wire and foil gages has the same form, its factor of proportionality is considerably less than for semiconductors, the ratio being about one to ten. While the sensitivity decreases, its variability with temperature, $d\pi_{st}/dT$, also diminishes with T, which constitutes a slight consolation for the inventor of compensating schemes. No one system has as yet been envisioned to cover the entire operating range of semiconductor elements. In the following, we describe an arrangement suggested by Mason for compensation over the range of $-70°$ to $+100°C$.

In the bridge circuit of Fig. 20, let the impressed voltage be E_1 and each of the branch resistors be a strain gage of zero-stress resistance R_0, which is, of course, temperature-dependent. Let R_6 be large and very constant. Then the expression for E_0, the voltage drop across the output resistor R_5, may be obtained in the simplified form given in Fig. 20, where ΔR is the change in gage resistance due to mechanical strain. If only R_5 were subjected to temperature variations but all other circuit

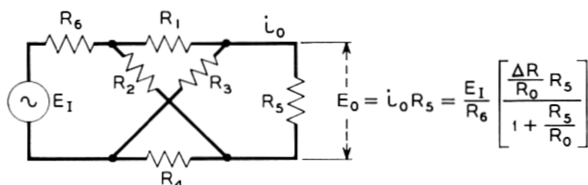

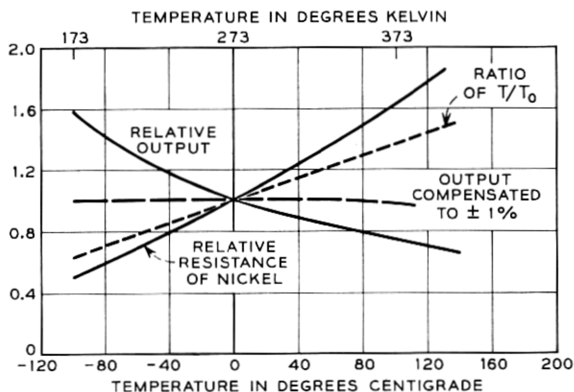

Fig. 20 — Proposed scheme for temperature compensation.

parameters were held fixed, its voltage output would be the ascending curve in Fig. 20. Conversely, thermal changes in $R_{1,2,3,4}$ would produce the descending curve for E_0. The formula indicates that proper choice of R_0/R_5 will provide a cancellation of these effects and will produce an output that is compensated within 1 per cent between $-70°$ and 100°C at a decrease in sensitivity by the factor 0.37. This may, for example, be accomplished with a nickel resistor for R_5.

V. CONCLUSIONS AND PROBLEMS FOR THE FUTURE

The foregoing discussions indicate that semiconductor materials show considerable promise for use in a variety of piezoresistive transducers. They are capable of handling both dc and ac signals and, due to a sensitivity about 70 times that of wire gages at room temperature, they eliminate the need for signal amplification in many situations. Their small dimensions permit subminiature embodiments for airborne applications and installations with severe space restrictions.

Some open questions regarding slippage and temperature compensation of these gages have already been pointed out in Section IV. To this list of current problems we add the need for adequate electrical filters to accompany the gages when their full sensitivity is to be utilized at minimum interference from noise. A final topic to be investigated is the resistance of such elements to mechanical shock and their fatigue characteristics under sustained vibrations.* Clearly, future efforts in the manufacture of dislocation-free semiconductor rods or the use of natural whiskers will have considerable bearing on this issue.

REFERENCES

1. Bridgman, P. W., Effect of Tension on the Resistance of Metals, Proc. Am. Acad. Arts Sci., **60,** 1925, p. 423.
2. Bridgman, P. W., The Effect of Homogeneous Mechanical Stress on the Electrical Resistance of Crystals, Phys. Rev., **42,** 1932, p. 858.
3. Allen, M., The Effect of Tension on the Electrical Resistance of Single Bismuth Crystals, Phys. Rev., **42,** 1932, p. 848.
4. Allen, M., The Effect of Tension on the Electrical Resistance of Single Antimony Crystals, Phys. Rev., **43,** 1933, p. 569.
5. Cookson, J. W., Theory of the Piezoresistive Effect, Phys. Rev., **47,** 1935, p. 194.
6. Allen, M., The Tension Coefficients of Resistance of Hexagonal Crystals Zinc and Cadmium, Phys. Rev., **49,** 1936, p. 248.
7. Allen, M., The Effect of Tension on the Electrical Resistance of Single Tetragonal Tin Crystals, Phys. Rev., **52,** 1937, p. 1246.
8. Lawrence, R., Temperature Dependence of Drift Mobility in Germanium, Phys. Rev., **89,** 1953, p. 1295.

---

* Some information on high-frequency fatigue endurance of silicon has been obtained by W. P. Mason with ultrasonic methods.

9. Smith, C. S., Piezoresistance Effect in Silicon and Germanium, Phys. Rev., **94,** 1954, p. 42.
10. Keyes, R. W., Temperature Dependence of the Elasto-resistance in N-Type Germanium, Phys. Rev., **100,** 1955, p. 1104.
11. Pearson, G. L., Read, W. T. and Feldmann, W. L., Deformation and Fracture of Small Silicon Crystals, Acta Metall., **5,** 1957, p. 181.
12. Bowers, R., Magnetic Susceptibility of Germanium, Phys. Rev., **108,** 1957, p. 683.
13. Morin, F. J., Geballe, T. H. and Herring, C., Temperature Dependence of Piezoresistance of High-Purity Silicon, Germanium, Phys. Rev., **105,** 1957, p. 525.
14. Pollack, M., Piezoresistance in Heavily Doped N-Type Germanium, Phys. Rev., **111,** 1958, p. 798.
15. Tuzzolino, A., Piezoresistance Constants of P-Type InSb, Phys. Rev., **109,** 1958, p. 1980.
16. Herring, C., Transport Properties of a Many-Valley Semiconductor, B.S.T.J., **34,** 1955, p. 237.
17. Herring, C. and Vogt, E., Transport and Deformation Potential Theory for Many-Valley Semiconductors with Anisotropic Scattering, Phys. Rev., **101,** 1956, p. 944.
18. Bateman, T. B. and McSkimin, H. T., private communication.
19. Burns, F. P., Piezoresistive Semiconductor Microphone, J. Acoust. Soc. Am., **29,** 1957, p. 248.
20. Mason, W. P., and Thurston, R. N., Piezoresistive Materials in Measuring Displacement, Force and Torque, J. Acoust. Soc. Am., **29,** 1957, p. 1096.
21. Sauer, H. A., Flaschen, S. S., and Hoesterey, T. C., Piezoresistance and Piezocapacitance Effects in Barium Strontium Titanate Ceramics, J. Am. Cer. Soc., **42,** 1959, p. 363.
22. Luer, H. L., private communication.
23. Courtney-Pratt, J. S. and Mason, W. P. private communication.
24. Forst, J. J. and Geyling, F. T., Applications of Semiconductor Transducers in Strain Gages and Rigid Dynamometers, Proc. Soc. Exp. Stress Anal., **17,** 1960, p. 143.
25. Mason, W. P., Semiconductors in Strain Gages, Bell Labs. Record, **37,** 1959, p. 7.
26. Dash, W. C., Growth of Silicon Crystals Free from Dislocations, J. App. Phys., **30,** 1959, p. 459.
27. Shockley, W., *Electrons and Holes in Semiconductors*, D. Van Nostrand Co., New York, 1950.